Investigating the Effects of Land Use Change on Subsurface, Surface and Atmospheric Branches of the Hydrologic Cycle in central Argentina

Sujan Pal[1], Francina Dominguez[1], Pablo Bollatti[2], Yi Yang[3], Javier Alvarez[4], Carlos Marcelo Garcia[4]

[1]Department of Atmospheric Sciences, University of Illinois at Urbana-Champaign, IL, USA.

[2]Instituto National de Technología Agropecuaria, Argentina.

[3]Department of Natural Resources and Environmental Sciences, University of Illinois at Urbana-Champaign, IL, USA.

[4]Institute for Advanced Studies for Engineering and Technology (IDIT CONICET-UNC) and Exact, Physical and Natural Sciences College, National University of Córdoba, (FCEFyN – UNC). 1611 Velez Sarsfield Ave, Córdoba, Argentina.

Corresponding author: Francina Dominguez (francina@illinois.edu)

Key Points:

- RELAMPAGO field observations and Noah-MP modeling are used to demonstrate that the fluxes of moisture and energy differ significantly between alfalfa and soy crops in central Argentina.
- Water table depth has significantly decreased, and runoff has increased over agricultural areas of central Argentina during the recent decades.
- Land cover changes partly explain regional changes in water table depth, runoff and Bowen ratio in central Argentina.

Abstract

Since the 1970s, agricultural production in central Argentina has shifted away from perennial crops and grasses towards annual crops, largely soy. In this work we use observations and modeling to understand how this shift in land cover has affected the sub-surface, surface and atmospheric fluxes of moisture and energy in a flat agricultural area. We analyze the flux tower data from a paired site at Marcos Juarez in central Argentina during the period of the RELAMPAGO field campaign (2018-2019). When compared to perennial alfalfa, the observations over soy show lower evapotranspiration and specific humidity, higher sensible heat, higher outgoing shortwave radiation and soil temperature. Furthermore, water table depth is shallower below the soy than the alfalfa sites. To better understand the long-term temporal behavior from 1970s to present, the Noah-MP land surface model was calibrated at both soy and alfalfa sites based on RELAMPAGO data. Long-term simulation of the calibrated model

suggests that ~95% of precipitation is evaporated in the alfalfa site with negligible recharge and runoff. In the case of soy, ET is about 68% of precipitation, leaving nearly 28% for recharge and 4% for runoff. Observed increases in streamflow and decreases in water table depth over time are likely linked to shifts in land cover. The changes in water table depth are enhanced in El Niño years. Furthermore, the partitioning of net radiation shifts from latent heat to sensible heat resulting in a 250% increase in Bowen ratio (from 0.2 to 0.7).

1. Introduction

During the 21st century, Argentina (Figure 1a) has experienced one of the fastest agricultural expansion rates in the planet (Baldi et al., 2008; Graesser et al., 2015). In many Argentinian regions, such as the province of Córdoba (Figure 1b), the past 60 years have seen a shift in agricultural production from one that had primarily perennial crops for livestock and grasses to one based on annual crops, largely dominated by soy, with confinement of livestock into feedlots. These changes came about due to a confluence of global and national factors. Technological advances in agricultural production such as the introduction of transgenic varieties, no-till farming, and crop rotation dramatically increased crop productivity in the region (Paruelo et al., 2005). Global economic shifts such as the increasing demand of soy-based and corn-based biofuels and the incursion of China, a large importer of soy-based products, into the World Trade Organization made it economically attractive for farmers to shift to soy and corn. At the national level, Argentinian protectionist policies of the early and mid-2000s significantly benefited the agricultural industry. As a result, in two decades (1995/96 to 2014/15), the cultivated area in regions such as Córdoba increased by 229%. Soy now dominates the landscape in the province of Cordoba accounting for nearly 60% of crops.

How can these dramatic changes in land use affect the hydrologic cycle? Some effects could parallel those of other regions of the globe that have experienced similar land use shifts, such as the Midwestern United States. In the US central region, European settlers arrived in the early to mid-19th century and by 1900 agriculture had become the dominant land use type, replacing the native grasses and forests of the region (Yaeger et al., 2013). Perennial and sod vegetation gave way to intensive corn and/or soybean crops with shorter summer growing seasons, which led to a decrease in evapotranspiration (ET). Decreased ET implied that more precipitation was going into groundwater recharge and routed into streams as baseflow (Zhang and Schilling, 2006). Furthermore, the ubiquitous use of tile drainage accelerates the lateral subsurface drainage of these systems (Yaeger et al., 2013). Several studies have attributed increased baseflow in the region to changes in land surface characteristics (Zhang and Schilling, 2006; Schilling et al., 2008; 2010; Xu et al., 2013).

The plains of the Pampas-Chaco in Argentina are flatter than their North American counterparts. They are sometimes referred to as hyperplanes, because their slopes are less than 0.1%, their drainage systems are poorly developed, and ET dominates the water balance (Jobbagy et al., 2008). Rodriguez et al., 2020 identified transpiration as the primary component of the water budget, followed by ET and interception, for dry forests and crops in the nearby region of San Luis. In general, their modeling results showed that liquid water fluxes here are strongly controlled by the vegetation cover. Giménez et al., 2020 illustrated that changes in land

77 cover from dry forests to crop reduced ET and increased intensity of deep drainage.
78 Consequently, changes in ET linked to agricultural practices can have dramatic consequences in
79 the water balance of the region. Measurements and remote-sensing estimates in Argentina show
80 that compared to annual crops,

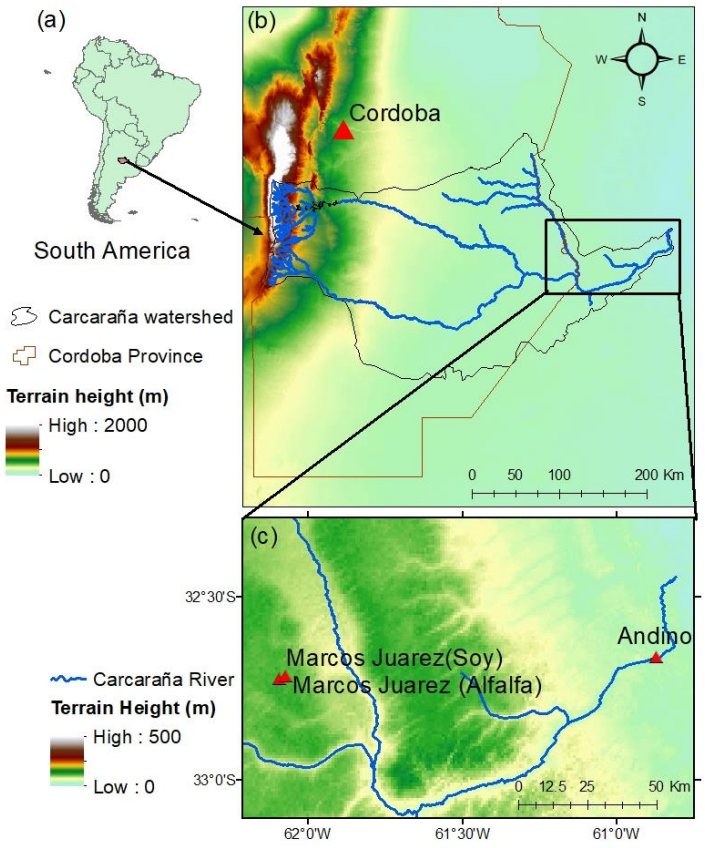

81

82 **Figure 1.** (a) Location of Carcarañá river basin in Argentina. (b) Elevation (m) and drainage
83 network of the basin. (c) Location of Marcos Juarez (paired sites) and Andino (streamflow
84 measurement location) within the watershed.

85 perennial crops such as alfalfa have deeper roots and year-round transpiration of more than 1000
86 mm/year compared to about 680 mm/year for single summer crops (Nosetto et al., 2015). Soil
87 moisture is usually higher, and the water table depth is closer to the surface below annual single
88 summer crops than in areas where perennial alfalfa is grown (Nosetto et al., 2012). Mercau et al.
89 (2015) suggests that at inter-annual timescales, the balance between precipitation and ET dictates
90 water table fluctuations, whereas crop choice can be a relevant control at intra-annual or seasonal
91 timescale. They also indicated that lateral transport of water, driven by hydraulic gradients
92 develops due to contrasting water consumption of different vegetation types. In a modeling study
93 Zellner et al. (2020) reach a similar conclusion, as climate was the main driver of water table
94 dynamics, but crops can influence water levels depending on the growing cycle. One of the

important consequences of changes in water table is related to flooding, as groundwater level is intimately related to the flooded area in the region (Viglizzo et al., 2009; Aragón et al., 2010). During periods of excess rains, the water table can reach the surface and cause "slow" floods that affect the region for several years (Kuppel et al., 2015). In fact, a modeling study by Lee et al., 2018 linked the increasing discharge of Parana river to land cover change using a terrestrial biosphere model.

Very few studies have relied on eddy covariance data in this region due to limited in-situ measurements. Garcia et al., 2017a provided estimates of CO_2 and water vapor fluxes, using eddy covariance measurements, in a dry forest of central Argentina. They identified that (1) the dry forest is a net sink of carbon, and (2) ET is the dominant vapor flux. In another study, Nosetto et al. (2020) compared the temporal patterns of CO_2 and water vapor fluxes of native dry forests and pastures at two different locations to show comparatively higher ET in the forests, primarily due to increased evaporating surface causing higher intercepted water. Long-term ground water table depth records are also limited in this region. Jobb*á*ggy et al., 2020 illustrated that unsaturated-saturated contact zone is a critical and dynamic hub of water partition using observed water table depth analysis at different vegetation. Clearly, this region shows strong interactions between land cover and terrestrial hydrology. However, there have not yet been any paired hydrometeorological observations of eddy-covariance estimates in the region, to understand how transient changes in land cover affect the partitioning of moisture and energy. Furthermore, the link between these differences and long-term trends in water table depth, hydrologic and atmospheric fluxes has not been established.

This study focuses on the regions surrounding Marcos Juarez (Figure 1c), a town located in the Carcarañá river basin in the Pampas region of Argentina, in central-southeast of C*ó*rdoba province. This region has experienced a dramatic transformation from mostly perennial grasses and alfalfa to annual (mostly soybean) cultivation (Figure 2) and is representative of the land-use changes in the region as a whole. Critically, the Argentinian National Institute for Agricultural Technology (INTA, for its acronym in Spanish) has an experimental alfalfa site and several soy sites in this location. Alfalfa is a perennial crop with characteristics similar to those that would have dominated the landscape in the 1970s, and soy crops are representative of the region at present. In addition, INTA has long-term water table depth observations (see section 2.1 and 3.1). We deployed two eddy covariance towers within the INTA site as part of the RELAMPAGO (Remote Sensing of Electrification, Lightning and Mesoscale/ Microscale Processes with Adaptive Ground Observations) field campaign which took place in west central Argentina (Nesbitt et al., 2016; Pal et al., 2021). The RELAMPAGO project consisted of an Extended Hydrometeorology Observing Period (EHOP) from 1 June 2018 to 30 April 2019. One of the goals of the EHOP is to understand how changes in land cover have affected the partitioning of rainfall between infiltration/runoff and impacted the residence times of soil moisture and groundwater in the Carcarañá Basin's terrestrial system. As part of the EHOP, the hydrometeorology team of RELAMPAGO installed thirty meteorological stations, including seven eddy covariance towers. The work we present in this manuscript is based on the two eddy covariance towers located within the INTA experimental site in Marcos Juarez Argentina (Figure 1).

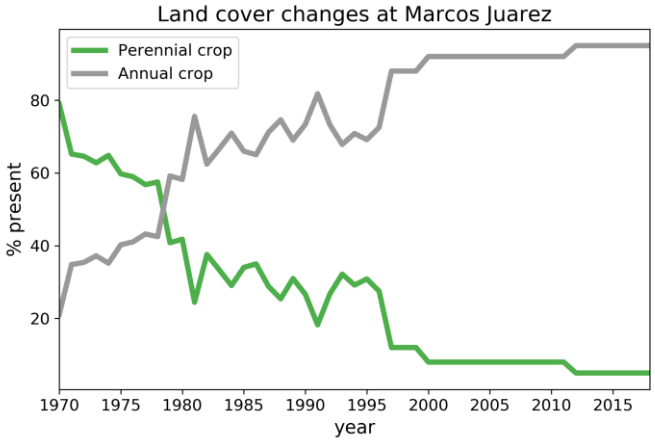

Figure 2. Evolution of land use change in Marcos Juarez, also representative of a large region of Argentina.

The goals of this manuscript are (1) to quantify the differences in energy and moisture fluxes between soy and alfalfa using high-resolution intra daily eddy covariance observations obtained from two RELAMPAGO flux towers, and (2) to understand the long-term effects of the gradual long-term shift from perennial to annual crops on surface, subsurface and atmospheric hydrology of the region with the help of a land surface model. The results from this study can be used to interpret long-term ET estimates in this region, which are also useful for INTA. Critically, the results from this study have implications for interpreting changes in water table depth based on land cover type and climate variability (such as El Niño and La Niña conditions). It is organized as follows: in section 2, the description of observed data, model specifications and the experimental design are discussed. In Section 3, the results are discussed and finally, the conclusions are summarized in Section 4. Additional information is provided in the Supporting Information (SI).

2. Materials and Methods

2.1 Long-term observations

Long-term measurements (1970-2020) of annual mean water table depth, precipitation and temperature were obtained from the agrometeorological station of the INTA Marcos Juárez. Annual runoff measurement from 1980 -2020 was obtained from the streamflow station at Andino (Figure 1c). The Carcarañá river drains an area of 60,000 km^2 at Andino (60.87W, 32.67S), which has long-term daily discharge information (Source: National Secretary of Water Resources). As such, Andino is downstream of Marcos Juarez as well as most of the Carcarañá river basin. Total runoff at Andino was further separated into baseflow and surface flow using Web-based Hydrograph Analysis Tool (WHAT) recursive digital filter method (Eckhardt, 2012). Throughout the text, significance is assessed using the Mann Kendall trend test at 95% significance level. Sequential Mann Kendall test (Sneyers, 1990; Modarres and Sarhadi, 2009) was used to detect breakpoints in discharge (see Figure S1 in SI).

2.2 RELAMPAGO 10-month observations

To understand the effect of different land use types on the fluxes of energy, moisture and momentum along the subsurface-surface and atmosphere continuum, the RELAMPAGO Hydrometeorology team installed two eddy covariance towers within the INTA experimental station in Marcos Juarez (Figure 1c). One of the towers was located within an alfalfa test plot (62° 4.492'W, 32° 42.970'S), while the other one was located in a soy site (62° 5.085'W, 32° 43.518'S; Figure 1c). RELAMPAGO flux measurements are part of the Integrated Surface Flux System (ISFS) (https://www.eol.ucar.edu/content/isfs-operations-relampago) maintained by the National Center for Atmospheric Research (NCAR) Earth Observing Laboratory (EOL). 3-D sonic anemometers and H_2O/CO_2 gas analyzers were used to measure net evapotranspiration and surface energy balance. As such, the sensible and latent heat fluxes were obtained from sonic anemometer measurements of vertical velocity, temperature and fast-response hygrometer measurements of water vapor density. Soil moisture sensors were installed at 5 cm depth. Radiation measurements were derived from the radiometers.

For this study, we analyze soil moisture (SM), sensible (SHF), latent heat fluxes (LHF, measured by the eddy covariance method), specific humidity (SH), outgoing shortwave radiation (OSR), soil temperature (ST), 2-m temperature (T2m), momentum in zonal and meridional direction (U- and V-momentum), and incoming shortwave radiation (ISR). The flux tower measurements were available from June 1, 2018 to April 1, 2019. However, good quality soil moisture data was only available from November 2018 to March 2019. Continuous groundwater measurements were obtained in the soy and alfalfa sites from both automated sensors and manual extraction by INTA and data was available from July 2018 to May 2019.

Our observations include the full crop planting-harvesting cycle. In Argentina, soy planting begins in September-October and planting ends in November, during the months of austral spring. December-February is the growing season (austral summer), and harvesting begins in March. Harvesting is completed by April-May. During the austral winter months, cover crops are sometimes planted to improve soil fertility and quality, as they were during the 2018-2019 season in Marcos Juarez.

2.3 Land surface modeling with Noah-MP

Land surface models compute the exchanges of water, heat, radiation and momentum between the land and atmosphere (Sellers et al., 1997; Zheng et al., 2019). In this study we use the Noah LSM (Chen and Dudhia, 2001) with multi-parameterization options (Noah-MP; Niu et al. 2011) run in a column (one-dimensional in the horizontal direction) configuration. Noah-MP calculates energy, water, and carbon dioxide fluxes between the biosphere and the atmosphere for different vegetation types, with closed energy budget and coupled water cycle. It has been previously implemented to investigate problems related to hydrologic cycle in standalone mode (Cai et al., 2014; Martinez et al. 2016a) and coupled with WRF (Martinez et al., 2016b; Pal et al., 2019) or WRF-Hydro (Gochis et al., 2018; Pal et al., 2021).

We use the Noah-MP land surface model in ‘offline’ mode with a groundwater scheme (Niu et al. 2007) to better understand the physical processes in the two sites with different vegetation and evaluate these processes for periods when we do not have observations (Figure 3a). The Ball-

Berry scheme was chosen for modeling stomatal resistance. Other parameterizations of Noah-MP were left as default; such as Monin-Obukhov scheme for surface layer drag, Jordan scheme for partitioning precipitation into rainfall and snowfall etc. (Niu et al., 2011). We do not analyze carbon fluxes in this work, so the carbon and dynamic vegetation module was not used. In the model, vegetation is represented by generic plant functional types, so the model needs to be calibrated regionally for best results. To better represent the soil state and ground water-soil moisture interaction, we modified the model soil column to have 14 layers (Table S1 in SI) extending from the surface to 4m below (following Miguez-Macho and Fan, 2012; Martinez et al., 2016a) while the default Noah-MP has only 2m deep soil column (with 4 layers).

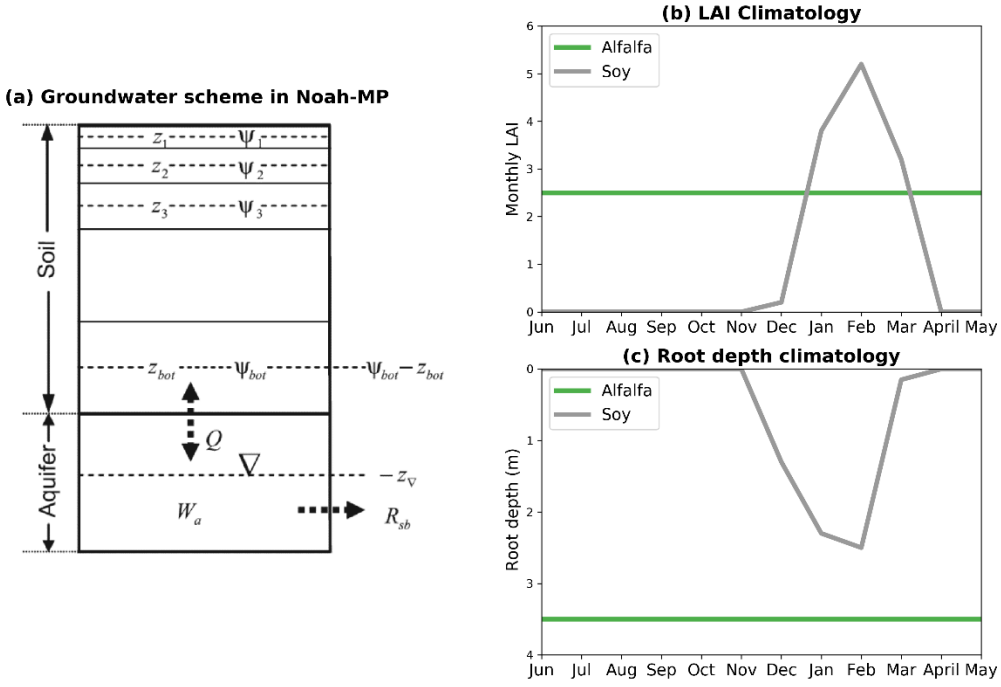

Figure 3. (a) Noah-MP groundwater model structure (adapted from Niu et al., 2007), z_i = height of soil layers, ψ = water head, Q = recharge rate (mms^{-1}), z_∇ = water table, bot = bottom layer, W_a = water stored in the aquifer (mm), R_{sb} = subsurface discharge (mms^{-1}), (b) LAI and (c) Root depth climatology used in the model simulation for Soy and alfalfa.

The model is run with prescribed atmospheric conditions from Global Land Data Assimilation System (GLDAS; Rodell et al., 2004) extracted for Marcos Juarez (nearest grid point from GLDAS). First, we performed two independent experiments named 'Noah-MP SOY' and 'Noah-MP ALFALFA' where the model configuration remains unchanged except for the vegetation parameters in the model. The vegetation parameters varied depending on the type of crop were 1) leaf area index (LAI), 2) root depth (RD), 3) maximum carboxylation rate (VMAX) in the Farquhar photosynthesis model (Farquhar et al., 1980), 4) the slope parameter (MP) and 5) the

intercept parameter (BP) in the Ball-Berry stomatal conductance model (Ball et al., 1987). VMAX, BP and MP controls the ET by controlling the stomatal resistance ($r_{s,i}$).

$$\frac{1}{r_{s,i}} = MP\frac{A}{c_{air}}\frac{e_{air}}{e_{sat}(T_v)}P_{air} + BP$$

Where 'A' is photosynthesis rates per unit LAI of leaves, which is controlled by VMAX. C_{air} is the CO_2 concentration at leaf surface, P_{air} is the surface air pressure. E_{air} and e_{sat} are vapor pressure at leaf surface and saturation vapor pressure at leaf surface temperature, respectively. Simulated ET is highly sensitive to these parameters of Noah-MP (Cuntz et al., 2016). Other vegetation parameters (e.g. leaf reflectivity, stem reflectivity, vegetation height, height of lower canopy bound etc.) for the Noah-MP ALFALFA and Noah-MP SOY simulations were kept as default Noah-MP values of 'Grasslands' and 'Croplands' modified IGBP MODIS 20-category vegetation, respectively. The soil type was taken as silty clay loam for both the sites.

The climatology of LAI and RD for the two vegetation types were obtained from literature (Figure 2 of Garcia et al. 2017b). Alfalfa grows during the whole year and have a deeper root system (3.5 m), while soy crops occupy the field only 4-5 months. In Noah-MP, we provided the root depth monthly climatology and prescribed monthly LAI climatology (Figure 3b, 3c) from Garcia et al., 2017b. As such, we did not use dynamic root or dynamic vegetation calculations. There are some remotely sensed LAI products available in this region, but they do not accurately represent the LAI climatology of these two specific vegetations, so we relied on this local literature reported LAI estimates. The two short-term simulations Noah-MP ALFALFA and Noah-MP SOY were performed to calibrate and validate the model at the two sites (see section 2.3.1 and section 3.3). The complete list of modeling experiments is presented in Table 1.

Table 1. List of experiments performed in this study.

Name of simulation	Simulation period	Vegetation	Forcing	Purpose
Noah-MP ALFALFA	June 1, 2018 – April 1, 2019	100% alfalfa	GLDAS	Calibration and validation
Noah-MP SOY	June 1, 2018 – April 1, 2019	100% soy	GLDAS	Calibration and validation
Noah-MP ALFALFA LT	January 1, 1970-December 31, 2018	100% alfalfa	GLDAS	Long term estimates of water budget and surface fluxes
Noah-MP SOY LT	January 1, 1970-December 31, 2018	100% soy	GLDAS	Long term estimates of water budget and surface fluxes

Using the calibrated model (see section 2.3.1) we performed two long-term simulations for 100% alfalfa and 100% soy conditions for the period January 1970 – April 2019 (Noah-MP ALFALFA LT and Noah-MP SOY LT, respectively in Table 1). The calibrated parameters for

the two vegetation types are used in the long-term simulations, and the GLDAS forcing for 1970-2019 is used to capture the interannual variability of the model inputs. These simulations provide components of annual water budget in the two different vegetation scenarios. It is worth mentioning here that these two scenarios are the two extremes of land use, and the actual transient land use would fall somewhere in between. However, this kind of experiment helps us understand the possible largest extent of transformation in hydrology due to land use change in this region. In our modeling experiment we do not take into account the effect of lateral flow (which might be generated by heterogeneous land cover) at inter-annual time scale. We spin up the model for 40 years for both scenarios and use the final SM and water table depth as the initial condition for the analyzed simulations.

2.3.1. Calibration

In Noah-MP, ET is most sensitive to the vegetation parameters VMAX, BP and MP (Cuntz et al., 2016). So, these parameters were obtained by calibration of the model based on RELAMPAGO flux tower observations of daily LHF at both the sites. All other parameters of the model were kept constant as the default configuration (section 2.3). The calibration was performed in a shuffle complex evolution method (Duan et al., 1993) minimizing the root mean square error (RMSE) of daily LHF data. Python SPOTPY package (Houska et al., 2015) was used to carry out the calibration. By this method, we can make realistic estimates of land surface variables at these two sites using Noah-MP (which previously had default generic crop parameters). The model was calibrated separately with respect to daily LHF data at both the sites to obtain the above-mentioned vegetation parameters. It is worth remembering here that our main goal from these modeling exercises is to obtain realistic water and energy balances for these two types of vegetations. LHF is a major part of both energy and water balance (as ET). Hence, we preferred to calibrate the model based on the common link (ET) of these two budget equations. The model was validated on the other variables during the same time period (June 1, 2018 – April 1, 2019) at those sites.

The results of calibration and validation is included in Table 2. For the soy (alfalfa) site, the parameters found were: VMAX = 132.425 (136.734), BP = 1580.63 (2041), MP = 6.89 (5.95). The model performance was validated against SHF and SM, at daily scale, at both the sites. The performance was significantly improved from the default parameter combinations, which underestimated the latent heat fluxes at both the sites. These calibrated parameters were used in the long-term simulations Noah-MP ALFALFA LT and Noah-MP SOY LT.

3. Results

3.1 Analysis of Long-Term Data

In 1970, the water table was nearly 11 m deep, however there has been a steady rise (statistically significant decreasing trend) of the water table and now it is approximately 2 m below ground at Marcos Juarez (Figure 4a). This trend does not seem to be related to climatic variables, e.g., precipitation and temperature. Annual mean precipitation shows a slight statistically non- significant decreasing trend (Figure 4b) and annual mean temperature shows a statistically

Table 2. Calibration and validation of Noah-MP at daily scale at the two sites. CC = correlation coefficient, RMSE = root mean square error.

		Alfalfa site		Soy site	
		CC	**RMSE**	**CC**	**RMSE**
Calibration	**Latent heat flux**	0.78	32.61	0.65	37.45
Validation	**Sensible heat flux**	0.62	24.62	0.64	20.1
	Top layer soil moisture	0.57	17.56	0.49	17.74

significant increasing trend (Figure 4c).

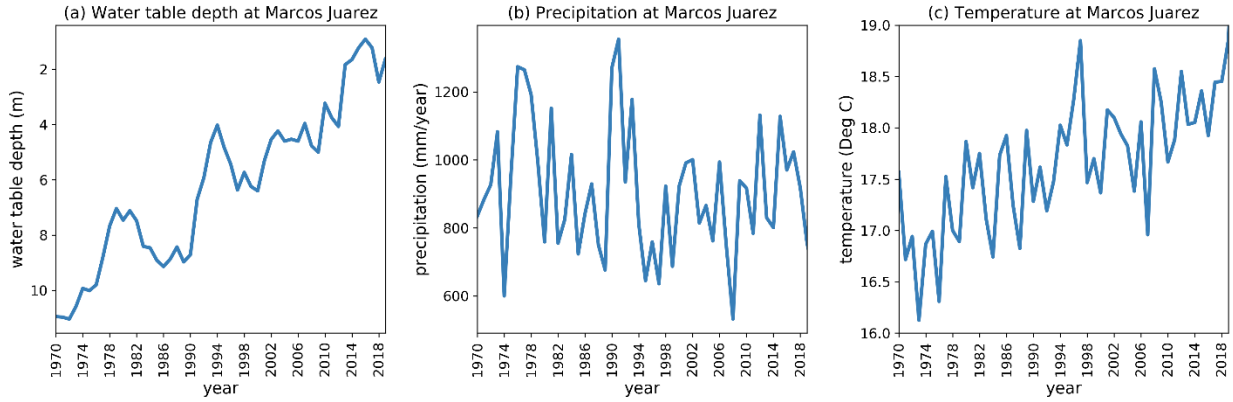

Figure 4. Long-term timeseries of annual mean (a) water table depth, (b) precipitation and (c) temperature at Marcos Juarez based on the Agrometeorological Station of the INTA Marcos Juárez and manual water table depth observations.

Streamflow at Andino has a statistically significant increasing trend, especially after 2000 (Figure 5). The increasing trend in total flow is result of both increased baseflow (statistically significant trend) and surface flow (statistically non-significant trend, Figure 5a). The year 2000 was found to be a year of change-point of trend (sequential Man-Kendall test, Figure S1 in SI). After 2000, baseflow has increased in the months of March and April; whereas surface flow has increased remarkably in February, March and October (Figure 5b). The combined effect of surface runoff and baseflow has resulted in the overall increase in streamflow at the Andino gauging station (Figure 5b-Figure 5d).

3.2 Analysis of the RELAMPAGO data

The analysis of the RELAMPAGO flux towers data is limited to the period June 1, 2018 to April 1, 2019 which corresponds to the EHOP. Figure 6 presents values at (1) sub-daily, (2) daily and (3) monthly timescale.

Hourly fluxes of sensible and latent heat in the soy and the alfalfa site show different characteristics. Diurnal cycles of LHF and SHF at both sites peak around 16 UTC (1 PM local

time, Figure 6a, 6d). The difference in magnitude is nominal at nighttime, and it increases during daytime. During most months, LHF (SHF) was higher at the alfalfa (soy) site than in the soy (alfalfa) site. The highest differences in the diurnal cycles of LHF (SHF) is found in December

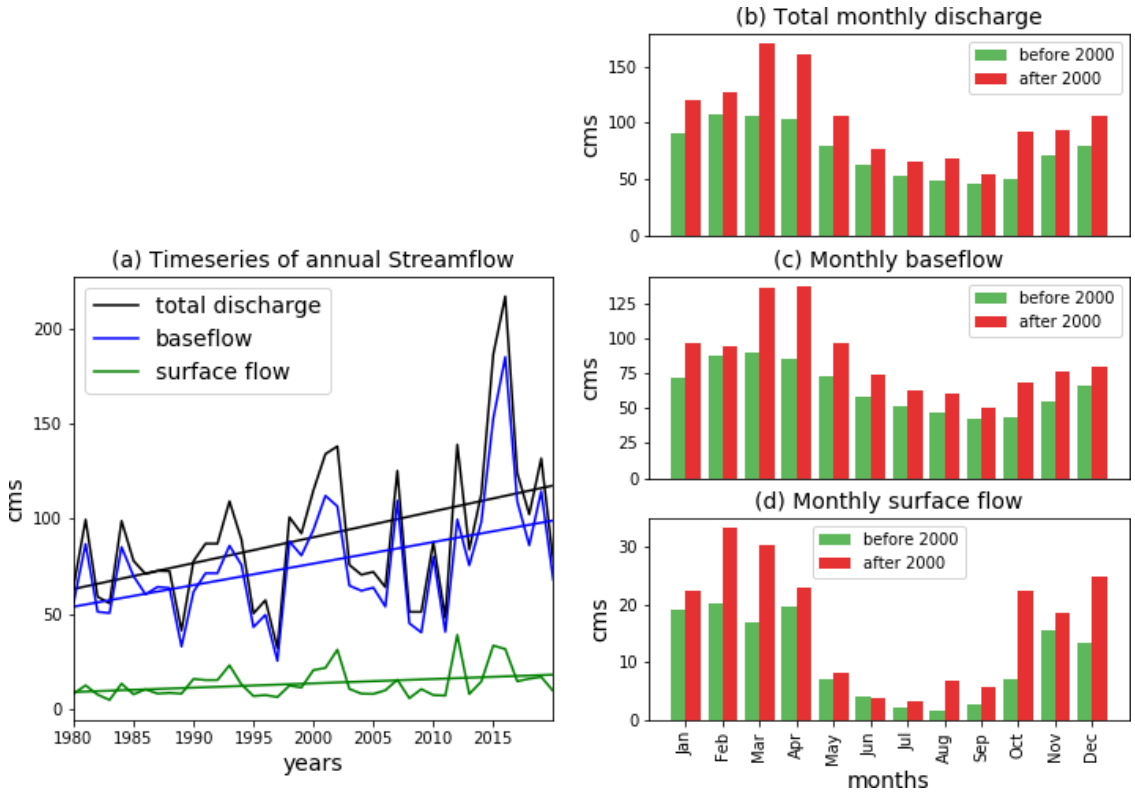

Figure 5. (a) Annual mean streamflow at Andino 1980-2016. Linear fit lines (solid straight lines) are also included. Monthly mean streamflow before and after 2000 separated into (b) total, (c) baseflow and (d) surface flow. cms = cubic meter per second.

(October). Sub-daily values of LHF (SHF) are comparable in the months of January and March (February and March). (2) Daily values of LHF are higher for alfalfa during most of the year, except for January, February and March, which correspond to the peak of the soy growing season when the annual crops are transpiring vigorously (Figure 6b and 6e). Daily values of SHF are much higher for Soy in all months, except February (Figure 6e). (3) Monthly mean values reinforce these facts (Figure 6c, 6f). LHF for alfalfa (soy) peaks in December (January). SHF for alfalfa (soy) peaks in February (December). This is related to the phenology of crops in this region (see section 2.2 and Figure 3b-3c). Crops transpire most during the end of growing season when they are mature. At the beginning of growing season, sensible heat is maximized. Based on our eddy covariance measurements, the accumulated 10-month ET of soy was found to be approximately 550 mm while for alfalfa it was around 880 mm.

In addition to sensible and latent heat, we analyzed specific humidity (SH), outgoing shortwave radiation (OSR), soil temperature (ST), T2m, U- and V-momentum and incoming shortwave radiation (ISR) measurements from the two sites. SH is higher at the Alfalfa site in all months except February and March at sub-daily, daily and monthly scale (Figure 7a-7c). The

difference is largest in January. This indicates that the atmosphere above alfalfa is more humid due to higher transpiration of the plants. OSR is higher at the Soy site in all months (Figure 7d-7f). This is likely related to higher albedo of Soy when compared to Alfalfa. This radiative effect alters the net incoming solar radiation. Soil temperature is higher at the Soy site in all months, except January and February (Figure 7g-7i), and this is linked to the higher SHF in the soy plot (Figure 6d-6f). No significant difference was found for T2m, U- and V-momentum and ISR (not shown). This indicates that thermodynamic properties are altered by the change in vegetation, but not the dynamic properties.

Water table is shallower at the soy site (Figure 8) by more than 1 meter and this difference increases in summer months when we see a sharp increase in water table following the first rains (November- February). We also see that the automated water table depth measurements (continuous line) agree with the manual observations (points). It is worth mentioning here that these measurements are critical in this region, as satellite estimates like GRACE fail to show the variation in water table depth (Figure S2 in SI), most likely due to its coarse resolution.

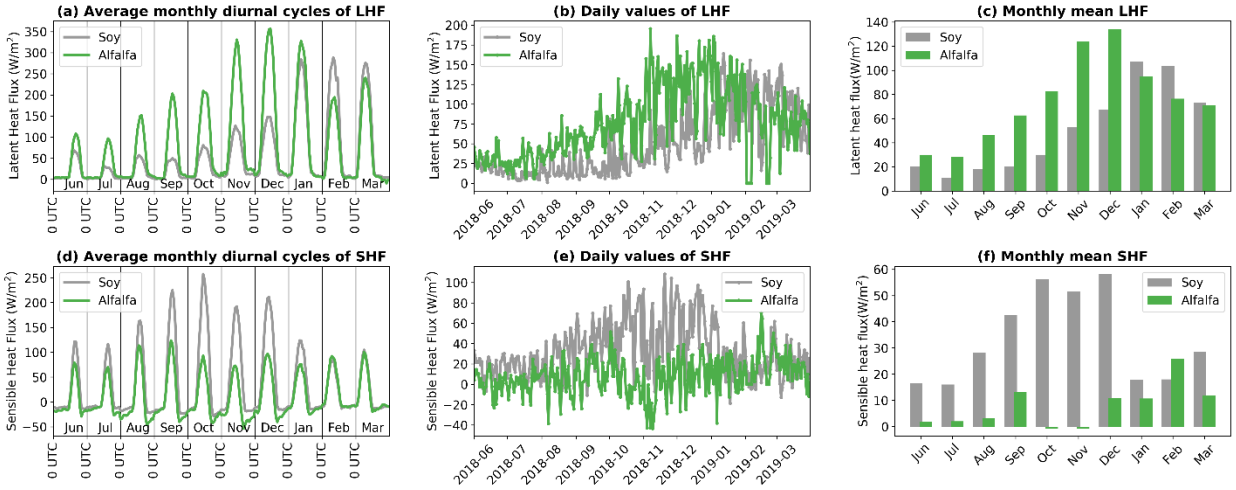

Figure 6. Diurnal, daily and monthly values of latent (a, b, c) and sensible heat flux (d, e, f) respectively at Marcos Juarez as observed by EOL towers during RELAMPAGO.

3.3 Model validation

When compared to observations, the Noah-MP calibrated model performs realistically for both the sites (Figure 9). LHF at the soy site was well represented by the model, except for some high daily values in October and December (Figure 9a). LHF at the alfalfa site was slightly underestimated during some days in the Spring and overestimated in the Summer months (Figure 9b). SHF was slightly underestimated by Noah-MP at the soy site and overestimated at the alfalfa site (Figure 9c, 9d). The model does a reasonable job (Figure 9e, 9f) in simulating the top layer SM (0-5cm), unfortunately we do not have SM observations until November of 2018. The discrepancies between model simulated fluxes and observations can be attributed to the simple structure of the Noah-MP model and calibration of limited variables within the model. Noah-MP assumes uniform soil with depth, uniform root distribution throughout the soil layers, ignores hydrologic redistribution which can play a role in modifying the amounts of SHF and LHF.

However, for the purposes of this study we are interested in comparing the representation of the two different vegetation types to understand the long-term effect of such changes in the fluxes of energy and moisture. Also, realistic land surface modeling complements the observations in terms of gap filling of missing values, which are common in these types of measurements.

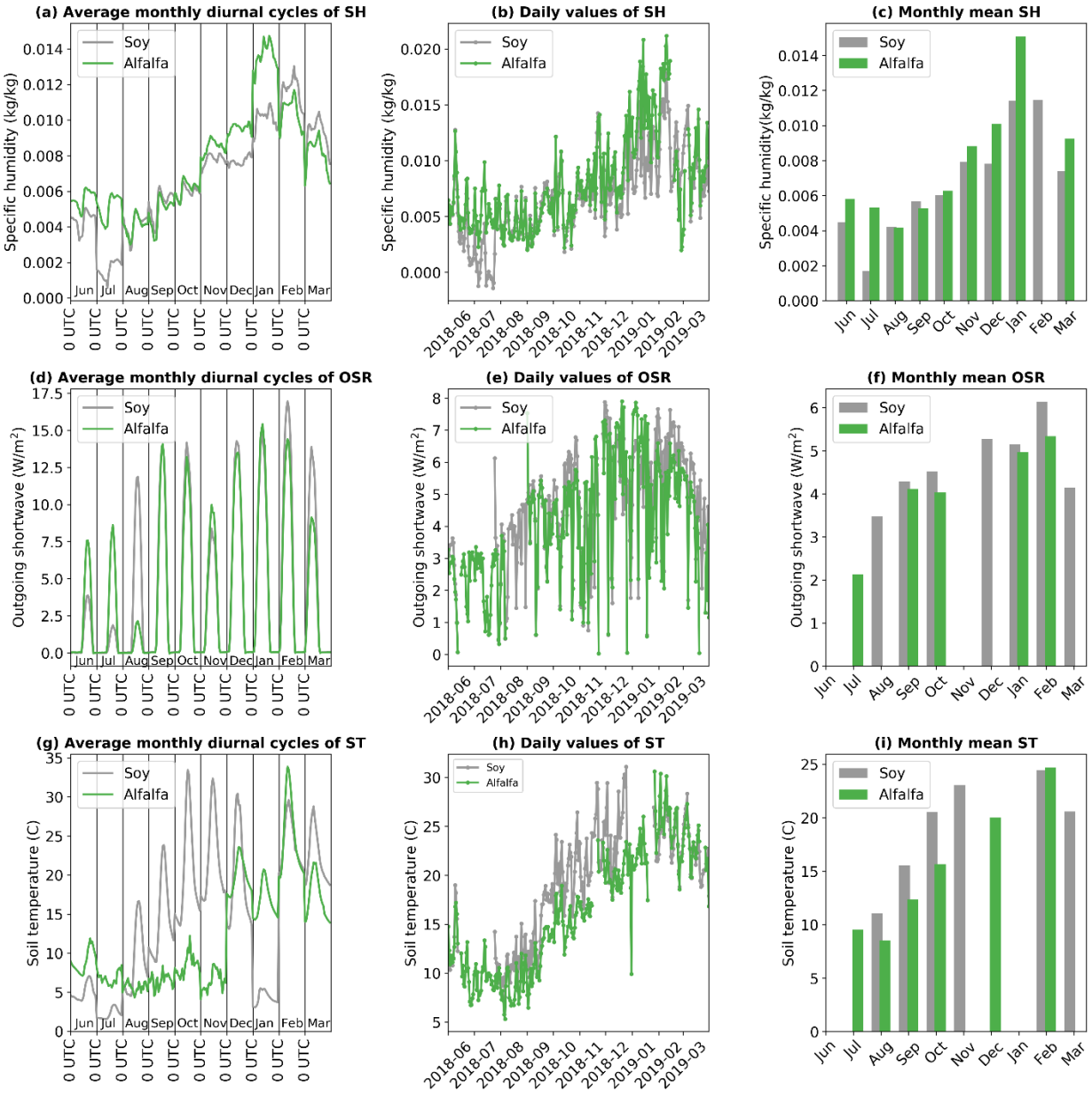

Figure 7. Diurnal, daily and monthly values of specific humidity (a, b, c), outgoing shortwave radiation (d, e, f) and soil temperature (g, h, i) respectively at Marcos Juarez as observed by EOL towers during RELAMPAGO.

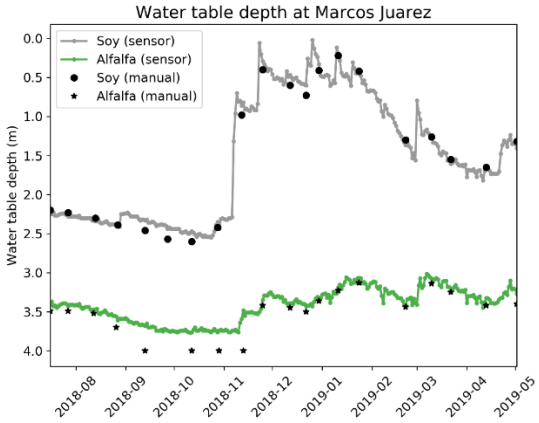

374

375 **Figure 8.** Water table depth at Marcos Juarez as measured by INTA during RELAMPAGO
376 period.

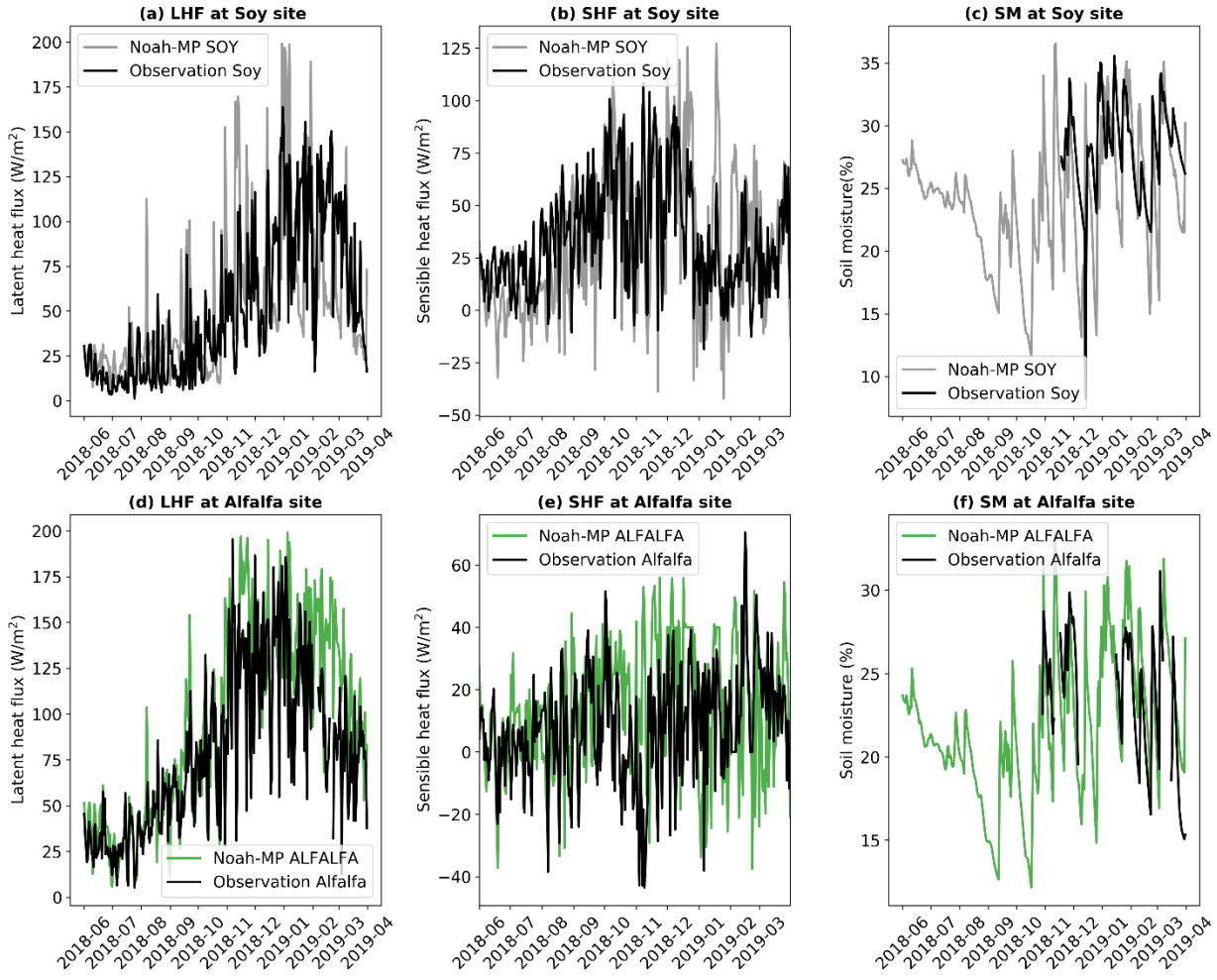

377

378 **Figure 9.** Calibrated Noah-MP model output at soy (a, b, c) and alfalfa site (d, e, f) as compared
379 with EOL flux tower observation during RELAMPAGO period. Missing/ unusual soil moisture
380 data is omitted from the plots.

3.4 Long-term water and energy balance of the two experiments

To understand how changes in agricultural practices might have changed the fluxes of water and energy, we performed two idealized long-term Noah-MP simulations for the period 1970-2018. In one simulation we set the land cover as soy (Noah-MP SOY LT, Table 1), while in the other simulation was alfalfa (Noah-MP ALFALFA LT, Table 1). Both simulations have the same atmospheric forcing for the 49-year period. The annual mean values of different components of the water budget (P = ET + R+ SR, where P = precipitation, ET = evapotranspiration, R = Recharge, SR = surface runoff, ignoring storage) of the two simulations are shown in Figure 10.

At the Alfalfa site, long-term average water balance reveals that ET is the dominant component (Figure 10a). Most of the incoming precipitation is evaporated (94.5%). Little goes into the aquifer as recharge (4.6%), along with negligible surface runoff (0.9%). This kind of partitioning of precipitation is realistic in this region (Rodriguez et al., 2020; Gim*é*nez et al., 2020). This is due to high evaporative potential of alfalfa, adequate water availability, and flatness of the region which results in very little surface runoff. The partitioning of incoming precipitation is different at the soy site (Figure 10b). In this case, a significant amount of precipitated water goes into aquifer as recharge (28.4%). This is a result of significantly less evaporation at the soy site (68.1%), when compared to alfalfa. The surface runoff component at the soy site is slightly higher (3.5%), but still negligible compared to the evaporation and recharge.

Hence, changing pasture to cropland results in four-fold increase in runoff and six-fold increase in deep recharge. These results are consistent with previous literature and observations (Nosetto et al, 2015; Rodriguez et al., 2020). The change in land use in this region results in more recharge, which contributes to a shallower water table depth and higher baseflow observed in recent years (Figure 3 and Figure 4). In other words, the moisture that would have entered the atmosphere in alfalfa vegetated region, is being accumulated below ground due to the shift in land use to soy. This shift in regime transforms the subsurface hydrology in terms of water table depth, baseflow and SM.

Analyzing the partitioning of available energy defined as the summation of latent heat flux (LHF) and sensible heat flux (SHF (Shuttleworth 1993), we find that LHF is the dominant surface flux component in both the vegetations (Figure 11). However, the balance is significantly different when comparing alfalfa and soy. LHF accounts for 85% of available energy over alfalfa while it accounts for 59% over soy. On the other hand, the 15% of the available energy over alfalfa goes into SHF, while it is 41% over soy. The Bowen ratio ($\frac{SHF}{LHF}$) reiterates this fact with mean of 0.2 over alfalfa and 0.7 over soy. Interestingly, there is a statistically significant increasing trend in Bowen ratio in the Noah-MP SOY LT simulation ($p = 0.014$), which is consistent with Zeng et al. 2020, and indicates a possible global warming signature further enhanced by agriculture. In other words, the recent atmosphere is having a significantly higher sensible heat flux in the spring and summer months, compared to previous decades and this is highlighted only in the soy simulation. This could also have a potential impact on the overlying

atmosphere, given this region is characterized by strong land-atmosphere coupling (Ruscica et al., 2015).

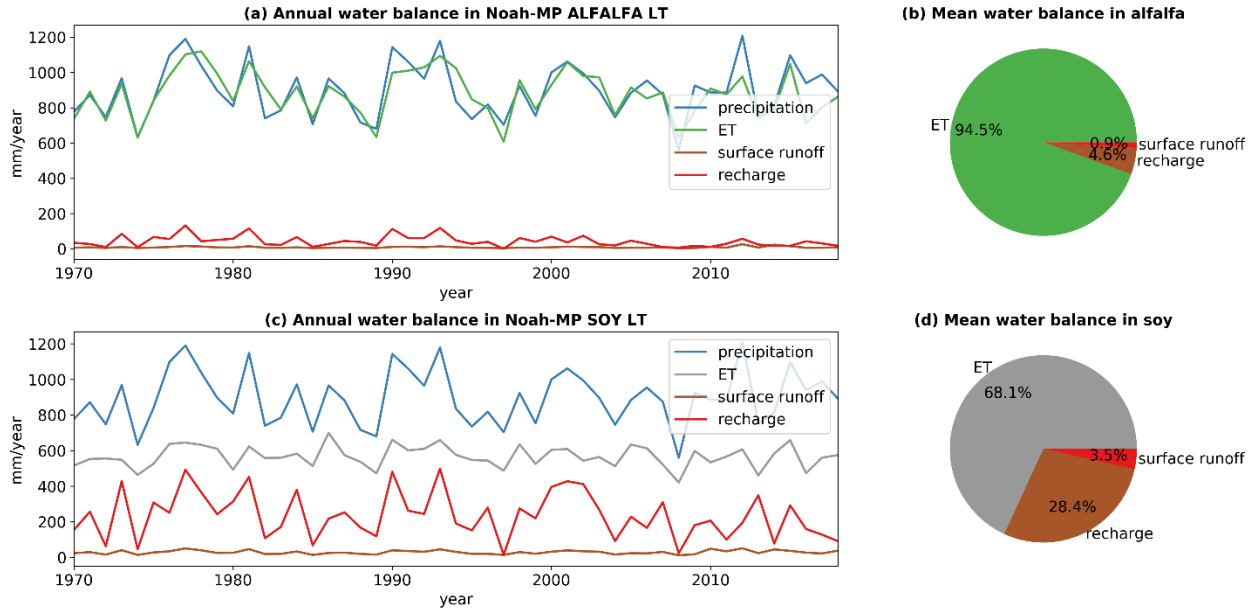

Figure 10. Long term annual estimates of precipitation, ET, runoff and recharge in (a) 100% alfalfa and (c) 100% soy simulations. Average partitioning of water in (b) alfalfa and (d) soy as calculated over the period 1970-2018.

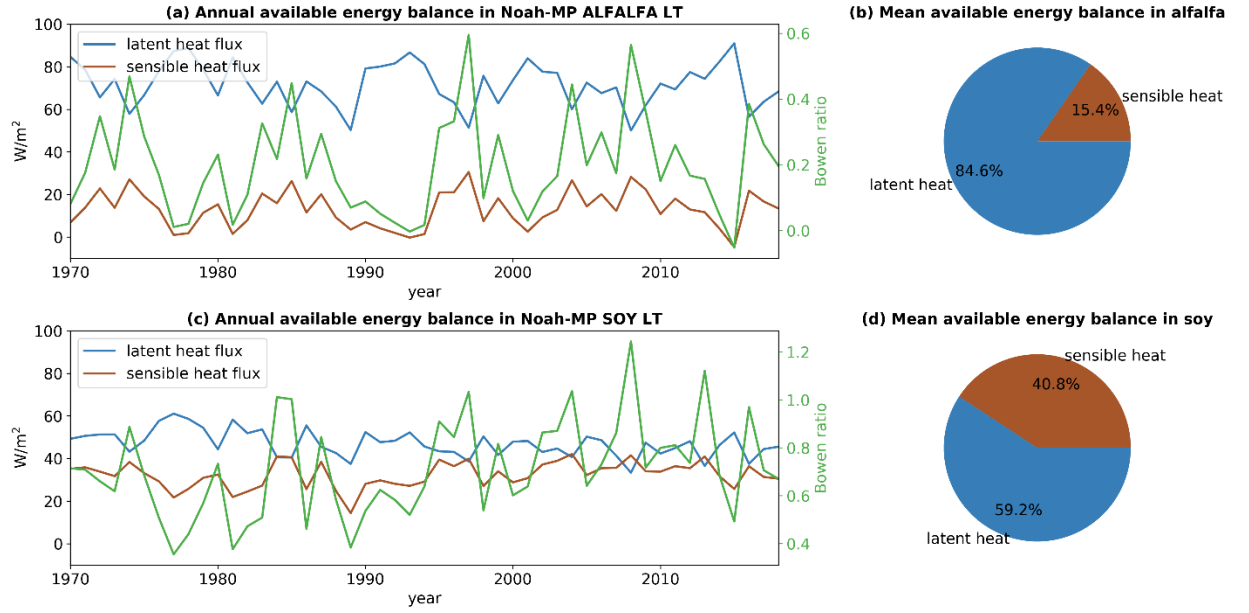

Figure 11. Long term annual estimates of LHF and SHF in (a) 100% alfalfa and (c) 100% soy simulations. Bowen ratio is shown with green line (secondary axis). Average partitioning of available energy in (b) alfalfa and (d) soy as calculated over the period 1970-2018.

3.5. Idealized transient land cover analysis

In the previous section, 100% soy and 100% alfalfa ideal simulations were used to estimate the long-term changes in the water fluxes. However, we would like to estimate the effect of a transient land cover which is similar to what happened historically (Figure 2). To estimate the transient moisture and energy fluxes, we used the yearly land cover changes for the region from Figure 2. It is important to highlight that, in reality, land cover in the region changed from mostly grasses and perennial crops like alfalfa, to a mixture of annual crops including soy, corn, wheat and other crops. Our simulations greatly simplify this complexity by assuming that the land cover is composed of a mixture of only alfalfa and soy. Furthermore, we do not account for the use of cover crops, despite the fact that these are sometimes used during the winter months. This will provide a first-order idea of the transient fluxes but will likely not reflect the actual historical conditions. The annual values were calculated based on a weighted "tile" approach commonly used in land surface models. For example, i^{th} year values of latent heat flux (LH_i) were calculated as

$$LH_i = \frac{LH_{alfalfa} * (\%\ alfalfa) + LH_{soy} * (\%\ soy)}{100}$$

This method was followed for other variables as well (Figure 12a-12d). The figures reveal that a gradual land use change pattern from alfalfa to soy, results in decreased LHF and increase SHF. Similarly, annual recharge and runoff increases over time. Our results show a decreasing trend of ET, increasing trend of SHF, increasing trend of annual recharge (not statistically significant), and increasing trend of surface runoff (not statistically significant). Nonetheless, these long-term trends agree in sign with the observations. Increased recharge and runoff are reflected in increased baseflow and storm flow of Carcarañá river (Figure 4). Along with decreasing water table depth, this poses a higher flooding risk in the region in recent years, which is reported in many studies (Aragón et al., 2010, Nosetto et al., 2012).

Finally, we argue that the change in water table depth over the years is partially linked to the transient recharge estimates. It is important to highlight that we are not directly simulating absolute values of water table depth because we lack information about the specific yield of the unconfined aquifer and because we cannot simulate lateral groundwater flow in the one-column Noah-MP configuration (Niu et al., 2007). Due to these uncertainties in the groundwater scheme, we can only infer how changes in the water table depth could be related to changes in recharge. We see a slight increase (not statistically significant) in annual recharge throughout the period (Figure 12c), and therefore, the simulated trend in recharge would not solely account for the 10m decrease in water table depth found in observations (Figure 4a). However, we find significant temporal correlation (R = 0.54) between interannual changes in water table depth change and transient recharge (Figure 13). This indicates that changes in recharge driven primarily by climate variability as represented by Noah-MP, correlate well with water table depth observations. This result agrees with Mercau et al. 2015, who related annual changes in water table depth to annual balance between precipitation and evaporation (P-E). However, these changes are also controlled by the type of vegetation. For example, changes in water table depth are more pronounced when there is soy rather than alfalfa (Figure 14). This is notable in the El Niño years (when precipitation is higher than normal in SESA, Cai et al., 2020). While alfalfa

can still use most of the excess water as ET, land planted with soy experiences comparatively larger changes in water table depth (with the help of more recharge, from Figure 13). This can pose a difference of as large as 1 m between these two vegetation types. In the La Niña years (precipitation below normal in SESA), vegetation las less impact on water table depth change, since less water is available for recharge. Hence, we conclude that interannual variability in recharge, and groundwater table depth are partially controlled by interannual climate variability and partially controlled by vegetation type. As such, the probability of large changes in water table depth during ENSO events is exacerbated when the land cover is switched from alfalfa to soy.

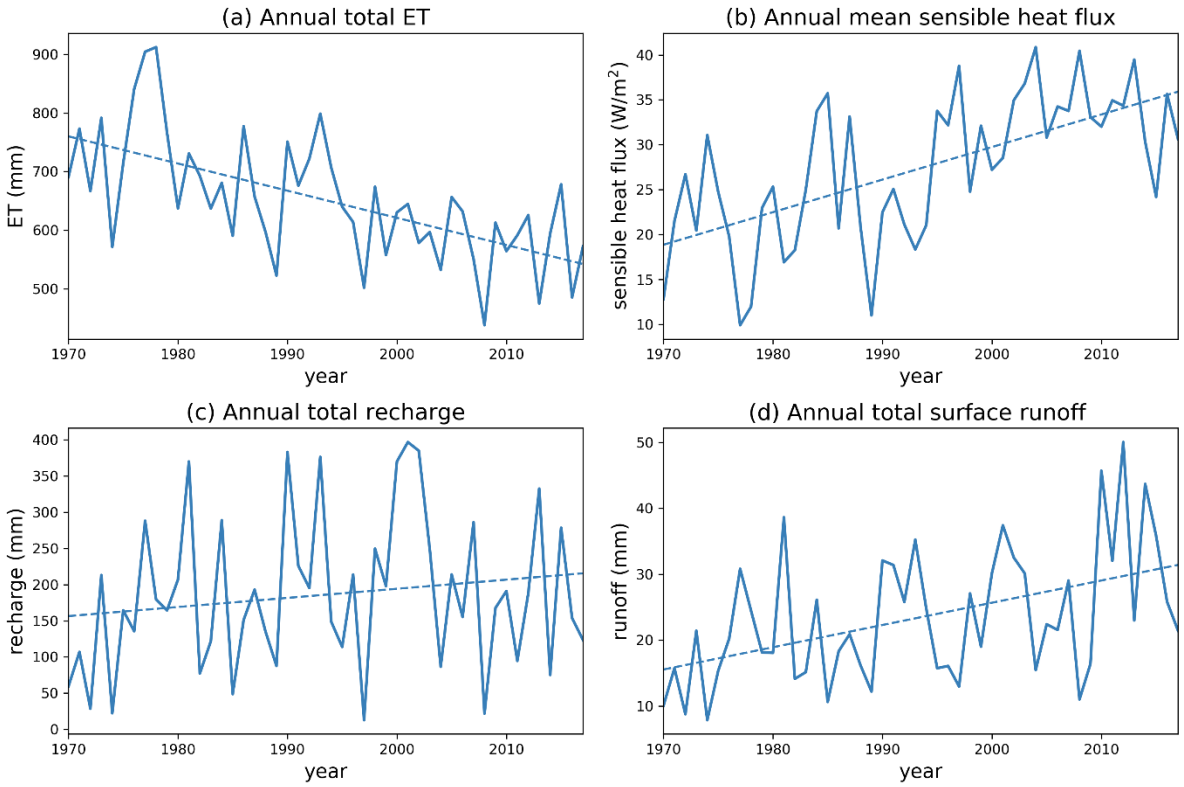

Figure 12. Long term estimates of annual mean (a) latent heat flux, (b) sensible heat flux (c) recharge (d) runoff and (e) water table depth according to the land use estimates of Figure 2. The dashed lines show the linear trends. Decreasing trend of ET was found statistically significant at 95% ($p = 6.6x10^{-6}$), increasing trend of SHF was found statistically significant at 95% ($p = 2.07x10^{-5}$), increasing trend of annual recharge was not found statistically significant at 95% ($p = 0.2665$), increasing trend of surface runoff was not found statistically significant at 95% ($p = 0.0016$).

4. Conclusions

In the past decades, there has been a dramatic shift of land cover in central Argentina from perennial to annual crops. These changes came about due to technological advances, global

economic shifts and national policies. In this work we use detailed observations and modeling to understand how the shift in land cover has also affected the sub-surface, surface and atmospheric fluxes of moisture and energy. Long-term observations have shown that, despite slightly decreasing precipitation, streamflow in the region has increased primarily due to baseflow. In addition, water table depth has decreased significantly since the 1970s. The RELAMPAGO field campaign provided us the opportunity to observe the hydrometeorology of the region using a paired eddy-covariance tower site in Marcos Juarez, Argentina. We installed the towers within the INTA experimental station which has an alfalfa experimental site along with soy crops. The alfalfa experimental site reflects conditions similar to those that prevailed in the 1970s, while the soy site is characteristic of the land cover of today.

Our observations reveal that ET and specific humidity are higher at the alfalfa site, particularly for the period of July-December. The alfalfa site also has deeper water table depth. On the other hand, sensible heat, outgoing shortwave radiation and soil temperature are higher at the soy site. The higher sensible heat in the soy crop between June and December is particularly striking. No significant differences were found in the other variables such as 2-m temperature, U- and V-momentum and incoming shortwave radiation. These observations were also used to calibrate Noah-MP land surface model parameters for this region.

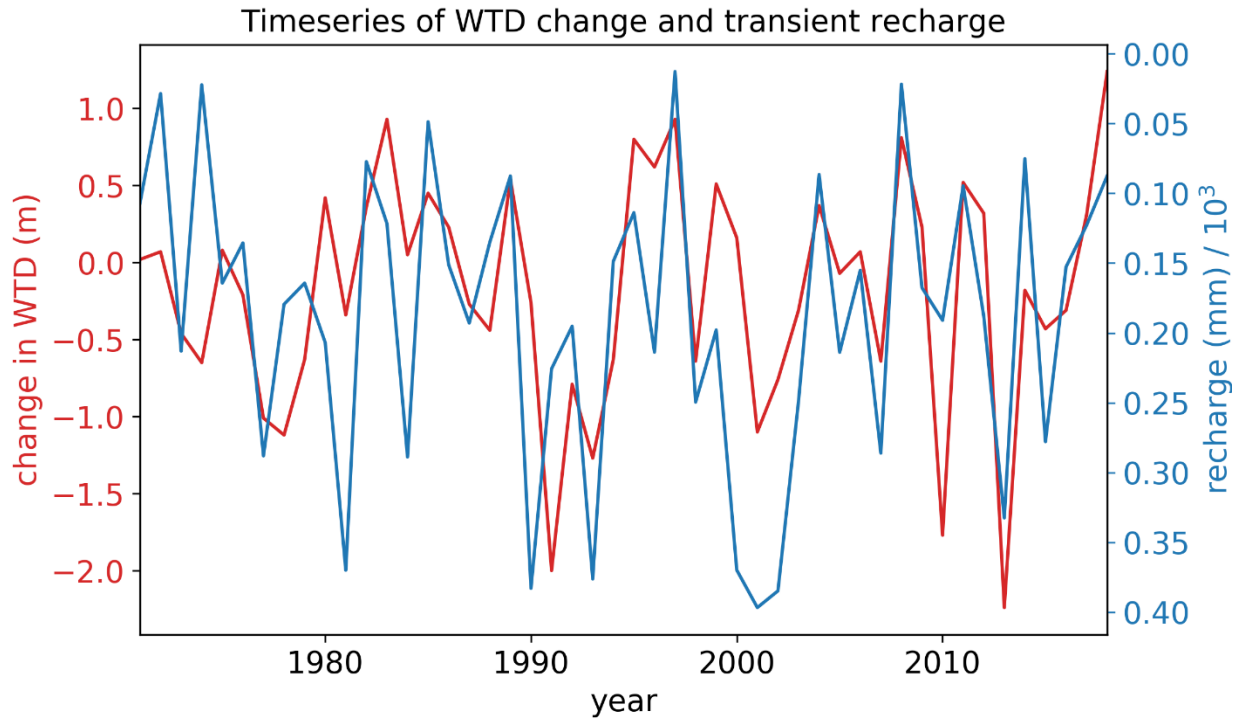

Figure 13. Timeseries of transient Noah-MP recharge and observed inter-annual variation in water table depth.

Long-term Noah-MP simulations reveal that different land-surface properties affect the partitioning of rainfall between ET, recharge and runoff. ET is significantly higher for alfalfa. Long term simulations reveal that ~95% of precipitation is evaporated in the alfalfa site with

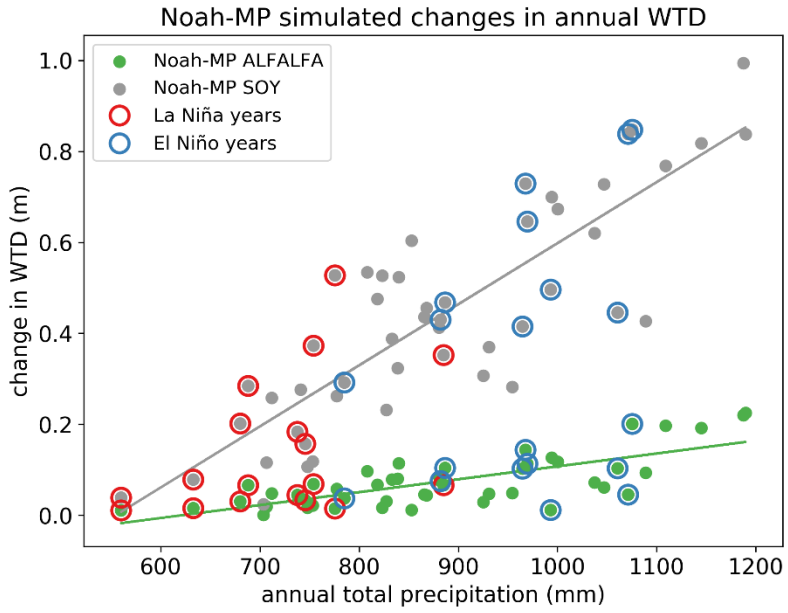

Figure 14. Effect of vegetation on the changes in WTD in different climatic years as simulated by Noah-MP. El Niño and La Niña years were identified based on Oceanic Niño Index (https://ggweather.com/enso/oni.htm). The solid lines show the linear trends in the data.

negligible recharge and runoff. On the other hand, ET in the soy site accounts for ~68% of precipitation. The recharge significantly increases in case of soy (~28% from ~5% in alfalfa). Runoff also increases from 0.9% in alfalfa to 3.5% in soy. Significantly higher recharge in soy would result in higher baseflow and shallower water table, as we have seen in the observations. However, the simulated increase in recharge in the transient simulation is not able to account for the dramatic observed change in water table depth. It is important to highlight that our experimental setup is highly simplified, with predefined LAI and root values and only one crop type in each simulation. More realistic estimates would require flux tower observations over other types of crops such as winter wheat, corn and cover crops. These land cover types likely have characteristic moisture and energy fluxes in between the soy and alfalfa. Furthermore, we do not explicitly simulate water table depth due to the fact that the one-dimensional model does not account for lateral groundwater flow and unknown aquifer related data. However, these results show that, given identical climate conditions, the different land covers result in a very different partitioning of precipitation. Higher recharge in the soy scenario contributes to higher water table depth and more runoff. The effect on water table depth is even more pronounced in El Niño years when higher than normal precipitation is available, and the soy scenario shows more significant changes in water table depth than the alfalfa scenario.

Our results suggest that the large-scale changes in land cover in Argentina have likely affected sub-surface, surface and atmospheric fluxes of moisture and energy. When compared to perennial land cover, annual crops such as soy result in a shallower and more variable water table, increased runoff driven by baseflow increases, decreased ET and increased sensible heat. In other words, much of the water that was going into the atmosphere in the 1970s is now going into the surface and subsurface. Furthermore, the energy that was being used to evaporate the water is now going into sensible heat, and this results in a dramatic 250% increase in the Bowen ratio. The implications of this shift in atmospheric fluxes of moisture and energy will be the focus of future work.

Acknowledgments, Samples, and Data

Support for this study has been provided by the National Science Foundation (NSF) Grant 1641167 “RELAMPAGO Hydrometeorology Component: Land Surface Controls on Heavy Precipitation and Flooding in the Carcarañá River Basin, Argentina”. Additional funding for Sujan Pal was provided by NSF CAREER Award (PI – Francina Dominguez) AGS 1454089 "Hydroclimatic Response to Natural and Anthropogenic Land Cover Change over South America: A Focus on the La Plata River Basin". The observed data sets, model inputs and model setup are stored at the github repository https://github.com/sujanpal/WRR_2021. We acknowledge NCAR EOL for collection, quality control and storage of RELAMPAGO data. We specially thank Steve Oncley (NCAR) for his help with data collection, quality control and processing. The authors declare no conflict of interest.

References

Aragón, R., E. G. Jobbágy, and E. F. Viglizzo (2010), Surface and groundwater dynamics in the sedimentary plains of the Western Pampas (Argentina), *Ecohydrol.*, 4(3), 433–447, doi:10.1002/eco.149.

Baldi G and Paruelo J M (2008), Land-use and land cover dynamics in South American temperate grasslands Ecol. Soc. 13 6

Ball, J.T., Woodrow, I.E., Berry, J.A., 1987. A Model Predicting Stomatal Conductance and its Contribution to the Control of Photosynthesis under Different Environmental Conditions, in: Progress in Photosynthesis Research. Springer Netherlands, Dordrecht, pp. 221–224. https://doi.org/10.1007/978-94-017-0519-6_48

Cai, W., McPhaden, M.J., Grimm, A.M. *et al.* Climate impacts of the El Niño–Southern Oscillation on South America. *Nat Rev Earth Environ* **1,** 215–231 (2020). https://doi.org/10.1038/s43017-020-0040-3

Cai, X., Z.-L. Yang, C. H. David, G.-Y. Niu, and M. Rodell, 2014: Hydrological evaluation of the Noah-MP land surface model for the Mississippi River Basin. J. Geophys. Res. Atmos., 119, 23–38, https://doi.org/10.1002/2013JD020792.

574 Chen, F., and J. Dudhia (2001), Coupling an advanced land surface-hydrology model with the
575 Penn State-NCAR MM5 modeling system. Part I: Model implementation and sensitivity, Mon.
576 Weather Rev., 129(4), 569–585.

577 Cuntz, M., J. Mai, L. Samaniego, M. Clark, V. Wulfmeyer, O. Branch, S. Attinger, and S.
578 Thober (2016),The impact of standard andhard-coded parameters on the hydrologic fluxes in the
579 Noah-MPland surface model, J. Geophys.Res. Atmos., 121, 10,676–
580 10,700,doi:10.1002/2016JD025097.

581 Duan, Q., V. K. Gupta, and S. Sorooshian (1993), Shuffled complex evolution approach for
582 effective and efficient global minimization, J. Optim. Theory Appl., 76(3), 501–521.

583 Eckhardt, K., 2012. Technical note: analytical sensitivity analysis of a two parameter recursive
584 digital baseflow separation filter. Hydrol. Earth Syst. Sci. 16,451–455.

585 Farquhar, G.D., von Caemmerer, S., Berry, J.A., 1980. A biochemical model of photosynthetic
586 CO2 assimilation in leaves of C3 species. Planta 149, 78–90.
587 https://doi.org/10.1007/BF00386231

588 García, A. G., Di Bella, C. M., Houspanossian, J., Magliano, P. N, Jobbágy, E. G., Posse, G., …
589 Nosetto, M. D. (2017a). Patterns and controls of carbon dioxide and water vapor fluxes in a dry
590 forest of Central Argentina. Agricultural and Forest Meteorology, 247,520–532.

591 García Pablo E., Angel N. Menénendez, Guillermo Podestá, Federico Bert, Poonam Arora &
592 Esteban Jobbágy (2017b) Land use as possible strategy for managing water table depth in flat
593 basins with shallow groundwater, International Journal of River Basin Management, 16:1, 79-
594 92, DOI: 10.1080/15715124.2017.1378223

595 Gochis, D.J., M. Barlage, A. Dugger, K. FitzGerald, L. Karsten, M. McAllister, J. McCreight, J.
596 Mills, A. RafieeiNasab, L. Read, K. Sampson, D. Yates, W. Yu, (2018). The WRF-Hydro
597 modeling system technical description, (Version 5.0). NCAR Technical Note. 107 pages.
598 https://ral.ucar.edu/sites/default/files/public/WRF-HydroV5TechnicalDescription.pdf, Source
599 Code DOI:10.5065/D6J38RBJ

600 Giménez, R, Mercau, JL, Bert, FE, et al. Hydrological and productive impacts of recent land-use
601 and land-cover changes in the semiarid Chaco: Understanding novel water excess in water scarce
602 farmlands. *Ecohydrology*. 2020; e2243. https://doi.org/10.1002/eco.2243

603 Graesser, J., T. M. Aide, H. R. Grau, and N. Ramankutty (2015), Cropland/pastureland dynamics
604 and the slowdown of deforestation in Latin America, *Environ. Res. Lett*., 10(3), 034017–11,
605 doi:10.1088/1748-9326/10/3/034017.

606 Houska, T., Kraft, P., Chamorro-Chavez, A. and Breuer, L.: SPOTting Model Parameters Using
607 a Ready-Made Python Package, PLoS ONE, 10(12), e0145180,
608 doi:10.1371/journal.pone.0145180, 2015.

Jobbagy Gampel, E. G., M. D. Nosetto, C. S. ssantoni, and G. Baldi (2008), El desafío ecohidrológico de las transiciones entre sistemas leñosos y herbáceos en la llanura Chaco-Pampeana, *Ecologia Austral*, 18, 305–322.

Jobbágy Esteban, Santiago Lorenzo, Ricardo Páez, et al. Plants vs. Streams: Their groundwater-mediated competition at "El Morro", a developing catchment in the dry plains of Argentina. *Authorea*. September 28, 2020. **DOI:** 10.22541/au.160133536.67833093

Kuppel, S., J. Houspanossian, M. D. Nosetto, and E. G. Jobbágy (2015), What does it take to flood the Pampas?: Lessons from a decade of strong hydrological fluctuations, *Water Resour Res*, 51(4), 2937–2950, doi:10.1002/2015WR016966.

Mercau Jorge L., Marcelo D. Nosetto, Federico Bert, Raúl Giménez, Esteban G. Jobbágy, Shallow groundwater dynamics in the Pampas: Climate, landscape and crop choice effects, Agricultural Water Management, Volume 163, 2016, Pages 159-168, ISSN 0378-3774, https://doi.org/10.1016/j.agwat.2015.09.013.

Lee, E., Livino, A., Han, SC. *et al.* Land cover change explains the increasing discharge of the Paraná River. *Reg Environ Change* **18,** 1871–1881 (2018). https://doi.org/10.1007/s10113-018-1321-y

Martinez, J. A., Dominguez, F., & Miguez-Macho, G. (2016a). Effects of a groundwater scheme on the simulation of soil moisture andevapotranspiration over southern South America.Journal of Hydrometeorology, 17, 2941–2957.https://doi.org/10.1175/JHM-D-16-0051.1

Martinez, J.A., F. Dominguez, and G. Miguezmacho. 2016b. Impacts of a groundwater scheme on hydroclimatological conditions over southern South America. J. Hydrometeorol. 17:2959–2978.https://doi.org/10.1175/JHM-D-16-0052.1

Miguez-Macho, G., and Y. Fan, 2012: The role of groundwater in the Amazon water cycle: 1. Influence on seasonal streamflow, flooding and wetlands. J. Geophys. Res., 117, D15113, doi:10.1029/2012JD017539.

Modarres, R., Sarhadi, A., 2009. Rainfall trends analysis of Iran in the last half of the twentieth century. J. Geophys. Res. 114.

National Secretary of Water Resources https://www.argentina.gob.ar/obras-publicas/hidricas/base-de-datos-hidrologica-integrada

Nesbitt, S. W., and Coauthors, 2016: RELAMPAGO Experimental Design Overview. Accessed 15 April 2020, https://www.eol.ucar.edu/field_projects/relampago.

Niu, G.-Y., Z.-L. Yang, R. E. Dickinson, L. E. Gulden, and H. Su (2007), Development of a simple groundwater model for use in climate modelsand evaluation with Gravity Recovery and Climate Experiment data,J. Geophys. Res., 112, D07103, doi:10.1029/2006JD007522.

Niu, G.-Y., et al. (2011), The Community Noah Land Surface Model withMulti-Parameterization Options (NOAH-MP): 1. Model description and evaluation with local-scale measurements, J. Geophys. Res., 116,D12109, doi:10.1029/2010JD015139.

Nosetto M.D., E.G. Jobbágy, A.B. Brizuela, R.B. Jackson, The hydrologic consequences of land cover change in central Argentina Agric. Ecosyst. Environ., 154 (2012), pp. 2-11

Nosetto, M. D., R. A. Paez, S. I. Ballesteros, and E. G. Jobbágy (2015), Higher water-table levels and flooding risk under grain vs. livestock production systems in the subhumid plains of the Pampas, *Agriculture, Ecosystems and Environment*, 206, 60–70, doi:10.1016/j.agee.2015.03.009.

Nosetto MD, Luna Toledo E,Magliano PN, Figuerola P, Blanco LJ, Jobbágy EG. Contrasting CO2 and water vapour fluxes in dry forest and pasture sites of central Argentina. Ecohydrology. 2020; e2244. https://doi.org/10.1002/eco.2244

Pal, S., H.-I. Chang, C. L. Castro, and F. Dominguez, 2019: Credibility of convection-permitting modeling to improve seasonal precipitation forecasting in the southwestern United States. Front Earth Sci., 7, 11, https://doi.org/10.3389/feart.2019.00011.

Pal, S., Dominguez, F., Dillon, M. E., Alvarez, J., Garcia, C. M., Nesbitt, S. W., & Gochis, D. (2021). Hydrometeorological Observations and Modeling of an Extreme Rainfall Event Using WRF and WRF-Hydro during the RELAMPAGO Field Campaign in Argentina, Journal of Hydrometeorology, 22(2), 331-351. doi: https://doi.org/10.1175/JHM-D-20-0133.1

Paruelo, J. M., J. P. guerschman, and S. R. Veron (2005), Expansion Agricola y cambios en el uso del suelo, Ciencia Hoy, 1–10.

Rodell, M., and Coauthors, 2004: The Global Land Data Assimilation System. Bull. Amer. Meteor. Soc., 85, 381–394, doi:10.1175/BAMS-85-3-381.

Rodriguez P., Raúl Giménez, Marcelo D. Nosetto, Esteban G. Jobbágy, Patricio N. Magliano, Changes in water fluxes partition related to the replacement of native dry forests by crops in the Dry Chaco, Journal of Arid Environments, Volume 183, 2020, 104281, ISSN 0140-1963, https://doi.org/10.1016/j.jaridenv.2020.104281.

Ruscica, R. C., Sörensson, A. A., & Meńendez, C. G. (2015). Pathways between soil moisture and precipitation in southeastern South America.Atmospheric Science Letters, 16(3), 267–272.

Sellers, P. J., et al. (1997), Modeling the exchanges of energy, water, and carbon between continents and the atmosphere, Science, 275 (5299),502–509.

Schilling, K. E., K.-S. Chan, H. Liu, and Y.-K. Zhang (2010), Quantifying the effect of land use land cover change on increasing discharge in the Upper Mississippi River, *Journal of Hydrology*, 387(3-4), 343–345, doi:10.1016/j.jhydrol.2010.04.019.

Schilling, K. E., M. K. Jha, Y.-K. Zhang, P. W. Gassman, and C. F. Wolter (2008), Impact of land use and land cover change on the water balance of a large agricultural watershed: Historical effects and future directions, *Water Resour Res*, 44(7), 563–12, doi:10.1029/2007WR006644.

Shuttleworth WJ. Evaporation. In: Maidment DR, ed. Handbook of Hydrology. New York: McGraw-Hill, Inc.; 1993, 4.1–4.53.

681 Sneyers, R., 1990. On statistical analysis of series of observation. Technical note No.143, WMO
682 No. 415. World Meteorological Organization, Geneva.

683 Viglizzo, E. F., E. G. Jobbágy, L. Carreño, F. C. Frank, R. Aragón, L. D. Oro, and V. Salvador
684 (2009), The dynamics of cultivation and floods in arable lands of Central Argentina, *Hydrol*
685 *Earth Syst Sc*, 13(4), 491–502, doi:10.5194/hess-13-491-2009.

686 Xu, X., B. R. Scanlon, K. Schilling, and A. Sun (2013), Relative importance of climate and land
687 surface changes on hydrologic changes in the US Midwest since the 1930s: Implications for
688 biofuel production, *Journal of Hydrology*, 497(C), 110–120, doi:10.1016/j.jhydrol.2013.05.041.

689 Yaeger, M. A., M. Sivapalan, G. F. McIsaac, and X. Cai (2013), Comparative analysis of
690 hydrologic signatures in two agricultural watersheds in east-central Illinois: legacies of the past
691 to inform the future, *Hydrol. Earth Syst. Sci*., 17(11), 4607–4623, doi:10.5194/hess-17-4607-
692 2013.

693 Zellner Moira, Guillermo A. García, Federico Bert, Dean Massey, Marcelo Nosetto, Exploring
694 reciprocal interactions between groundwater and land cover decisions in flat agricultural areas
695 and variable climate, Environmental Modelling & Software, Volume 126, 2020, 104641, ISSN
696 1364-8152, https://doi.org/10.1016/j.envsoft.2020.104641.

697 Zeng, J., Zhang, Q. The trends in land surface heat fluxes over global monsoon domains and
698 their responses to monsoon and precipitation. *Sci Rep* **10,** 5762 (2020).
699 https://doi.org/10.1038/s41598-020-62467-0

700 Zhang, Y. K., and K. E. Schilling (2006), Increasing streamflow and baseflow in Mississippi
701 River since the 1940s: Effect of land use change, *Journal of Hydrology*, 324(1-4), 412–422,
702 doi:10.1016/j.jhydrol.2005.09.033.

703 Zheng, H., Yang, Z. L., Lin, P. R., Wei, J. F., Wu, W. Y., Li, L. C., et al. (2019). On the
704 sensitivity of the precipitation partitioning into evapotranspiration and runoff in land surface
705 parameterizations. Water Resources Research, 55,95–111.
706 https://doi.org/10.1029/2017WR022236

707

708

709